

Inflation as a prediction of loop quantum cosmology

Linda Linsefors*

*Laboratoire de Physique Subatomique et de Cosmologie, UJF, INPG, CNRS, IN2P3
53, avenue des Martyrs, 38026 Grenoble cedex, France*

Aurelien Barrau†

*Laboratoire de Physique Subatomique et de Cosmologie, UJF, INPG, CNRS, IN2P3
53, avenue des Martyrs, 38026 Grenoble cedex, France*

(Dated: January 8, 2013)

Loop quantum cosmology is known to be closely linked with an inflationary phase. In this article, we study quantitatively the probability for a long enough stage of slow-roll inflation to occur, by assuming a minimalist massive scalar field as the main content of the universe. The phase of the field in its "pre-bounce" oscillatory state is taken as a natural random parameter. We find that the probability for a given number of inflationary e-folds is quite sharply peaked around 145, which is indeed more than enough to solve all the standard cosmological problems. In this precise sense, a satisfactory inflation is therefore a clear prediction of loop gravity. In addition, we derive an original and stringent upper limit on the Barbero-Immirzi parameter. The general picture about inflation, super-inflation, deflation and super-deflation is also much clarified in the framework of bouncing cosmologies.

PACS numbers: 04.60.-m 98.80.Qc

I. INTRODUCTION

Loop quantum gravity (LQG) is a tentative nonperturbative and background-independent quantization of general relativity. It uses Ashtekar variables, namely $SU(2)$ valued connections and conjugate densitized triads. The quantization is obtained through holonomies of the connections and fluxes of the densitized triads (see, *e.g.*, [1] for an introduction). Basically, loop quantum cosmology (LQC) is the symmetry reduced version of LQG. In LQC, the big bang is generically replaced by a big bounce due to huge repulsive quantum geometrical effects (see, *e.g.*, [2] for a review).

Two main LQG corrections are expected when dealing with a semiclassical approach, as will be the case in this study, which is mostly devoted to potentially observable effects. The first one comes from the fact that loop quantization is based on holonomies, *i.e.* exponentials of the connection rather than direct connection components. The second one arises for inverse powers of the densitized triad, which, when quantized, becomes an operator with zero in its discrete spectrum, thus lacking a direct inverse. As the status of "inverse volume" corrections is not fully clear, due to the fiducial volume cell dependence, this work focuses on the holonomy term which has a major influence on the background equations. The emphasis is put on LQC as this model provides a well defined framework, with known and controlled equations of motion. Most results are, however, probably quite generic to bouncing models.

After reviewing the formalism, we derive the probability density function for the number of e-folds. This study is complementary to the ones performed in [3] where the probability distribution was assumed to be flat and defined at the bounce. Here, we make a very different assumption: the phase of the field oscillating in the remote past is considered to be the most natural random variable. We don't use any heavy machinery and rely only on very minimalistic hypotheses. Nor do we consider different possible conditions at the bounce, as in [3], but instead derive them explicitly as predictions of the model.

In addition, we show that, if the critical density is assumed to be a free parameter, a stringent upper limit on the Barbero-Immirzi parameter, γ , that is the free parameter of loop gravity, can be obtained. This is especially important if, as suggested in [4], the entropy of black holes can be recovered for any γ , therefore leaving its value mostly unconstrained.

II. FRAMEWORK

The LQC-modified Friedman equation reads as

$$H^2 = \frac{\kappa}{3}\rho \left(1 - \frac{\rho}{\rho_c}\right). \quad (1)$$

The main content of the universe is assumed to be a massive scalar field ϕ with mass m fulfilling:

$$\ddot{\phi} + 3H\dot{\phi} + m^2\phi = 0. \quad (2)$$

Except in the last section, we use the critical density, *i.e.* density at the bounce, given by [2] $\rho_c = \sqrt{3}m_{\text{Pl}}^4/(32\pi^2\gamma^3) \simeq 0.41m_{\text{Pl}}^4$, where $\kappa = 8\pi G$ and $\gamma = 0.2375$.

*Electronic address: linsefors@lpsc.in2p3.fr

†Electronic address: Aurelien.Barrau@cern.ch

We define the fractions of potential and kinetic energy, normalized to the maximum energy density:

$$x := \frac{m\phi}{\sqrt{2\rho_c}} \quad \text{and} \quad y := \frac{\dot{\phi}}{\sqrt{2\rho_c}}, \quad (3)$$

so that

$$\rho = \rho_c (x^2 + y^2). \quad (4)$$

The equations of motion for x , y and ρ are:

$$\dot{x} = my, \quad \dot{y} = -my - 3Hy, \quad (5)$$

$$\dot{\rho} = -6H\rho_c y^2. \quad (6)$$

Trying to confront LQG with the real world is a key issue. Many works have been devoted to the computation of power spectra and their subsequent comparison with observations (see, *e.g.*, [5]). Here, we don't follow this track but, in the spirit of [3], focus instead on the "probability" of the universe being like it is within the loop gravity framework. This probability is not obvious to interpret. However, it clearly says something about the "naturalness" of the model.

III. PHASES OF THE LQC BOUNCING UNIVERSE

Using Eq. (1) and Eqs. (4)-(6), the evolution of the universe can be generically described by five phases:

- A. Pre-bounce oscillations
- B. Slow-roll deflation
- C. Super-deflation, bounce and super-inflation
- D. Slow-roll inflation
- E. Post-bounce oscillations

We assume that ρ_c is large enough so that $\rho \ll \rho_c$ is always the last of the relevant conditions to be violated before the bounce and the first one to be restored after the bounce. In the following equations t is always the cosmic time but it will be shifted between solutions for the different phases.

The calculations behind the results in this section are presented in appendix A.

A. Pre-bounce oscillations

This phase is characterized by the fact that x and y are oscillating with vanishing mean values and growing amplitudes. In this study, we naturally assume this phase to be the initial state of the bouncing universe. The conditions for pre-bounce oscillations are:

$$\rho \ll \rho_c, \quad H < 0, \quad H^2 \ll m^2. \quad (7)$$

The evolution in this phase can be approximated by:

$$\rho = \rho_0 \left(1 - \frac{1}{2} \sqrt{3\kappa\rho_0} \left(t + \frac{1}{2m} \sin(2mt + 2\delta) \right) \right)^{-2}, \quad (8)$$

$$x = \sqrt{\frac{\rho}{\rho_c}} \sin(mt + \delta), \quad y = \sqrt{\frac{\rho}{\rho_c}} \cos(mt + \delta). \quad (9)$$

This is stable until ρ grows large enough to violate the last condition.

B. Slow-roll deflation

Slow-roll deflation is characterized by an almost constant y and a linearly growing $|x|$. The probability of slow-roll deflation is small, since it occurs only if the relation between x and y is very specific at the end of the phase of pre-bounce oscillations. Slow-roll deflation is unstable. The conditions for Slow-roll deflation are:

$$\rho \ll \rho_c, \quad H < 0, \quad H^2 \gg m^2, \quad x^2 \gg y^2. \quad (10)$$

In this phase, the equation of motion for y can be approximated by:

$$\dot{y} = \sqrt{3\kappa\rho_c} |x| \left(y - \text{sign}(x) \frac{m}{\sqrt{3\kappa\rho_c}} \right). \quad (11)$$

The value $y = \text{sign}(x) \frac{m}{\sqrt{3\kappa\rho_c}}$ is an unstable stationary point. The variable y will evolve away from $\text{sign}(x) \frac{m}{\sqrt{3\kappa\rho_c}}$. However, if y starts out very close to $\text{sign}(x) \frac{m}{\sqrt{3\kappa\rho_c}}$ then $\dot{y} \approx 0$ for a while, and this leads to slow-roll deflation.

C. Super-deflation, bounce and super-inflation

This phase is characterized by a large $|y|$ and a rapidly growing or decreasing x (y , and therefore \dot{x} do not change sign during this phase). Super-deflation starts directly after post-bounce oscillations or after slow-roll deflation. The conditions for this phase are:

$$H^2 \gg m^2, \quad y^2 \gg x^2. \quad (12)$$

The evolution can be approximated by:

$$\rho = \rho_c (1 + 3\kappa\rho_c t^2)^{-1}, \quad y = \pm (1 + 3\kappa\rho_c t^2)^{-1/2}, \quad (13)$$

$$x = x_B \pm \frac{m}{\sqrt{3\kappa\rho_c}} \text{arcsinh} \left(\sqrt{3\kappa\rho_c} t \right), \quad (14)$$

where $t = 0$ at the bounce for Eqs. (13)-(14). This phase is stable for $H < 0$ but unstable for $H > 0$ since, in the later case, $|y|$ is decreasing rapidly and will eventually violate the second condition of Eqs. (12).

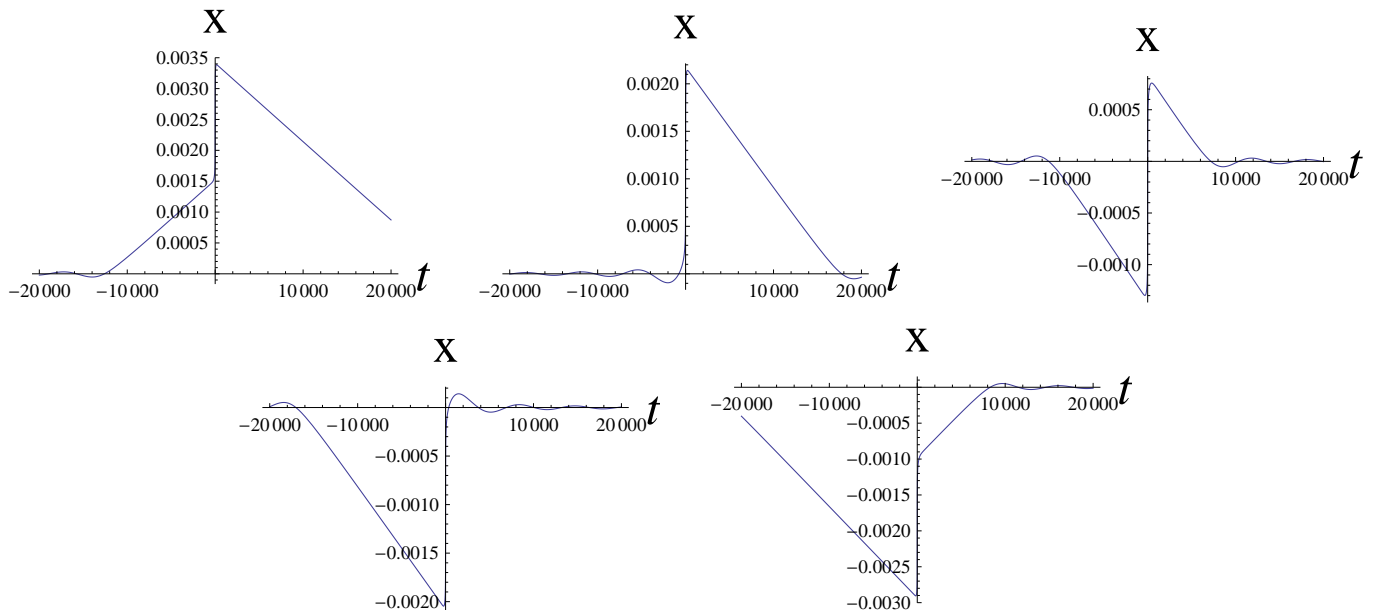


FIG. 1: Some typical plots for x as a function of time: Type I (upper left), Type II (upper middle), Type III (upper right), Type IV (lower left) and Type V (lower right). The mass of the scalar field is $m = 10^{-3}$ but the features remain true for any mass.

D. Slow-roll inflation

Slow-roll inflation happens if the second condition of Eq. (12) is broken before the first one. This is usually the case. The conditions for slow-roll inflation are:

$$\rho \ll \rho_c, H > 0, H^2 \gg m^2, x^2 \gg y^2. \quad (15)$$

In this phase, the equation of motion for y can be approximated by:

$$\dot{y} = -\sqrt{3\kappa\rho_c}|x| \left(y + \text{sign}(x) \frac{m}{\sqrt{3\kappa\rho_c}} \right), \quad (16)$$

which should be compared with Eq. (11). In this case $y = -\text{sign}(x) \frac{m}{\sqrt{3\kappa\rho_c}}$ is an attractor, therefore Slow-roll inflation is stable until one of the two last conditions is violated, which occurs at approximately the same value of x for both conditions.

E. Post-bounce oscillations

The conditions for post-bounce oscillations are:

$$\rho \ll \rho_c, H > 0, H^2 \ll m^2. \quad (17)$$

The evolutions in this phase can be approximated by:

$$\rho = \rho_0 \left(1 + \frac{1}{2} \sqrt{3\kappa\rho_0} \left(t + \frac{1}{2m} \sin(2mt + 2\delta) \right) \right)^{-2}, \quad (18)$$

together with Eqs. (9).

IV. PARAMETERS AND CLASSES OF EVOLUTION

At the bounce $x^2 + y^2 = 1$; the parameters for the solutions can therefore be taken to be x_B and $\text{sign}(y_B)$. Only the relative sign between x_B and y_B is physical. We choose $\text{sign}(y_B) = 1$ without loss of generality. The solutions can be divided into five classes:

Type I: Longer slow-roll inflation than slow-roll deflation, x does not change sign around the bounce.

Type II: Slow-roll inflation but no slow-roll deflation.

Type III: Both slow-roll inflation and slow-roll deflation with opposite signs of x .

Type IV: Slow-roll deflation but no slow-roll inflation.

Type V: Longer slow-roll deflation than slow-roll inflation, x does not change sign around the bounce.

Typical plots of x for each class of solutions are shown in Fig. 1. This fully clarifies the different possible scenarios in effective LQC.

V. TYPICAL BEHAVIORS AND PROBABILITIES

In this section, the probabilities for different evolutions, from random initial conditions set in the pre-bounce oscillation phase, are calculated. In this phase, the evolution of the universe is described by Eqs. (8)-(9),

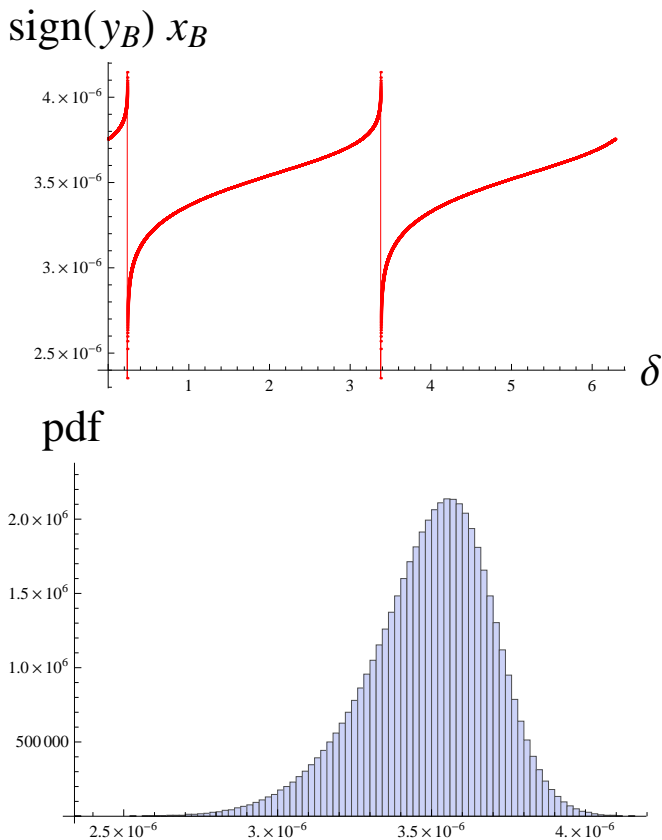


FIG. 2: $\text{sign}(y_B)x_B$ as a function of δ (upper plot) and its probability distribution (lower plot). The mass of the scalar field is $m = 1.21 \times 10^{-6}$, as favored by observations.

with parameters ρ_0 and δ . However, the transformation

$$\begin{aligned} \rho_0 &\rightarrow \rho_1 \\ \delta &\rightarrow \delta - \frac{2m}{\sqrt{3\kappa\rho_1}} \left(1 - \sqrt{\frac{\rho_1}{\rho_0}}\right) \\ t &\rightarrow t + \frac{2}{\sqrt{3\kappa\rho_1}} \left(1 - \sqrt{\frac{\rho_1}{\rho_0}}\right) \end{aligned} \quad (19)$$

will not change the solution, allowing us to take δ as the only parameter. In addition, a flat probability distribution for δ will be preserved over time, making it a most natural choice. Assuming such a distribution for δ , and choosing ρ_0 so that the solution is initially well approximated by Eqs. (8)-(9), the probability of different x_B can be calculated numerically using the full Eqs. (1) and (4)-(5) (we project the result down to the physically relevant parameters by considering $\text{sign}(y_B)x_B$). The value of $\text{sign}(y_B)x_B$ as a function of δ and the resulting probability distribution are showed in Fig. 2.

The probability of $\text{sign}(y_B)x_B$, previously taken as unknown, is in fact highly peaked around 3.6×10^{-6} . This corresponds to solutions of Type II, as could be expected from the arguments given in the previous section. Luckily, this also corresponds to a strong kinetic energy domination at the bounce (therefore backreaction effects can be more safely neglected [6]).

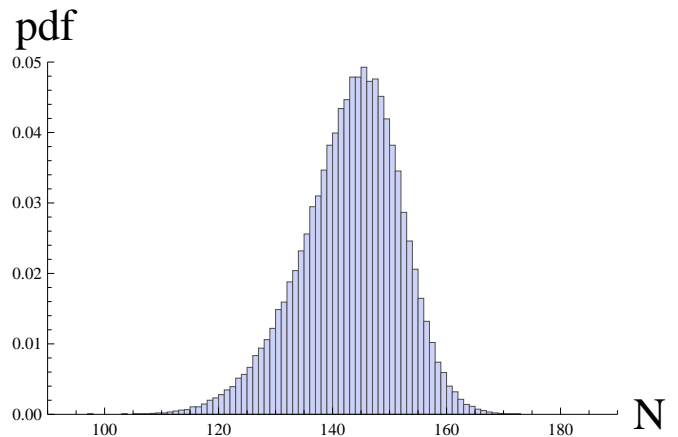


FIG. 3: Probability density of the number of e-folds during slow-roll inflation. The mass of the scalar field is $m = 1.21 \times 10^{-6}$.

In this case, slow-roll inflation starts at $|x| = x_{\max} := \max(|x|)$, which is related to the length of slow-roll inflation by $N = \frac{\kappa\rho_c}{2} \left(\frac{x_{\max}}{m}\right)^2 \simeq 5.1 \left(\frac{x_{\max}}{m}\right)^2$, where N is the number of e-folds during slow-roll inflation. The probability density for N is given in Fig. 3, showing that the model nearly unavoidably leads to a long enough phase of inflation. This becomes an important prediction of LQC: inflation and its duration are not arbitrary in the model.

A raw analytical estimate for N can also be easily obtained by assuming that the phase of superdeflation, bounce and super-inflation starts at $H = -m$ and $x = 0$, and ends at $H = m$. One then finds that $x_{\max} = \frac{2m}{\sqrt{3\kappa\rho_c}} \ln\left(\frac{2}{m}\sqrt{\frac{\kappa}{3}\rho_c}\right)$, where we have used $\text{arcsinh}\left(\frac{1}{m}\sqrt{\frac{\kappa}{3}\rho_c}\right) \approx \ln\left(\frac{2}{m}\sqrt{\frac{\kappa}{3}\rho_c}\right)$. This leads to

$$N = \frac{2}{3} \ln\left(\frac{2}{m}\sqrt{\frac{\kappa}{3}\rho_c}\right)^2, \quad (20)$$

which agrees very well with numerical mean values.

VI. CONSTRAINTS

So far, we have used the standard value of ρ_c , with a Barbero-Immirzi parameter γ assumed to be known from black hole entropy (see, *e.g.*, [7]). By instead taking ρ_c as a free parameter, we can constrain ρ_c and γ . Previous attempts to constrain ρ_c (see [8]) from cosmological data were based on $x_{\max} < 1$. However, we have shown that, in all realistic cases, $x_{\max} \ll 1$.

We can derive an upper limit on γ by requiring a large enough probability for a long enough slow-roll inflation. Fig. 4 shows $P(N > 65)$ as a function of ρ_c and Table I gives the constraints on ρ_c and γ for different required minimum probabilities for $N > 65$ (one can also perform an analytical calculation using Eq. (20), leading to $\rho_c < 1.6 \times 10^{-5}$). Basically, the result is that γ should be

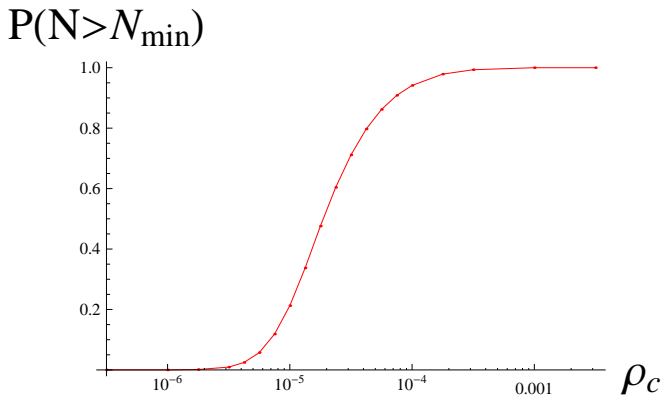


FIG. 4: Probability for having more than 65 e-folds of slow-roll inflation, $P(N > 65)$, as a function of ρ_c . The mass of the field is $m = 1.21 \times 10^{-6}$.

$P(N > 65)$	ρ_c	γ
0.5	1.9×10^{-5}	6.6
0.05	5.4×10^{-6}	10.1
0.01	3.2×10^{-6}	11.9

TABLE I: Lower bound on ρ_c and upper bound on γ for different probabilities for slow-roll inflation longer than 65 e-folds.

smaller than 10.1 at 95% confidence level and smaller than 11.9 at 99% confidence level. This is much more stringent than previous cosmological constraints [8]: $\gamma < 1100$.

VII. CONCLUSION

This letter establishes that a long enough slow-roll inflationary phase is nearly unavoidable in LQC. The preferred value is $N = 145$ e-folds, this is a prediction of the model. Values lower than 100 or greater than 170 are highly non-probable. In addition, the value of x_B , the square root of the fraction of potential energy at the bounce, is no longer unknown but is shown to be very close to 3.5×10^{-6} . Finally, the Barbero-Immirzi parameter is now bounded to be smaller than 10-12 (depending on the confidence level), which is, by far, the best cosmological constraint.

Appendix A: Derivation of evolutions in the different phases

In this appendix we present the calculations behind the results in section III.

1. Oscillations

These calculations apply to both pre- and post-bounce oscillations.

The first condition of Eq. (7) and Eq. (17) ensure that we can approximate Eq. (1) by:

$$H = \pm \sqrt{\frac{\kappa}{3}} \rho. \quad (\text{A1})$$

In addition, the last condition of Eq. (7) and Eq. (17) ensures that we can approximate x and y by oscillating functions with frequency m and varying amplitudes. This, together with Eq. (4) gives Eq. (9). From this, Eq. (6) can be simplified to:

$$\dot{\rho} = \mp 2\sqrt{3\kappa} \cos^2(mt + \delta) \rho^{3/2}, \quad (\text{A2})$$

which can be integrated to give Eq. (8) and Eq. (18).

2. Slow-roll

These calculations apply to both slow-roll deflation and slow-roll inflation.

The last condition of Eq. (10) and Eq. (15) ensures that we can approximate Eq. (4) by:

$$\rho = \rho_c x^2. \quad (\text{A3})$$

This, together with Eq. (1) and the first condition of Eq. (10) and Eq. (15) gives

$$H = \pm \sqrt{\frac{\kappa}{3}} \rho_c |x|, \quad (\text{A4})$$

so that the second part of Eq. (5) becomes Eq. (11) or Eq. (16).

3. Super deflation, bounce and superinflation

Without approximations, Eq. (1) can be written as:

$$H = \pm \sqrt{\frac{\kappa}{3} \rho \left(1 - \frac{\rho}{\rho_c}\right)}. \quad (\text{A5})$$

The second condition of Eq. (12) ensures that we can approximate Eq. (4) by

$$\rho = \rho_c y^2. \quad (\text{A6})$$

Using the two above equations, Eq. (6) can be simplified to:

$$\dot{\rho} = \mp 2\sqrt{3\kappa} \left(1 - \frac{\rho}{\rho_c}\right) \rho^{3/2}, \quad (\text{A7})$$

which can be integrated to give Eq. (13), which is true both before and after the bounce. Integrating the first part of Eq. (5), using the second part of Eq. (13) gives Eq. (14).

-
- [1] P. Dona & S. Speziale, arXiv:1007.0402V1; A. Perez, arXiv:gr-qc/0409061v3; R. Gambini & J. Pullin, *A First Course in Loop Quantum Gravity*, Oxford, Oxford University Press, 2011; C. Rovelli, arXiv:1102.3660v5 [gr-qc]; C. Rovelli, *Quantum Gravity*, Cambridge, Cambridge University Press, 2004; C. Rovelli, *Living Rev. Relativity*, 1, 1, 1998; L. Smolin, arXiv:hep-th/0408048v3; T. Thiemann, *Lect. Notes Phys.*, 631, 41, 2003; T. Thiemann, *Modern Canonical Quantum General Relativity*, Cambridge, Cambridge University Press, 2007
- [2] A. Ashtekar, M. Bojowald and J. Lewandowski, *Adv. Theor. Math. Phys.* 7, 233, 2003; A. Ashtekar, *Gen. Rel. Grav.* 41, 707, 2009; A. Ashtekar, P. Singh, *Class. Quantum Grav.* 28, 213001, 2011; M. Bojowald, *Living Rev. Rel.* 11, 4, 2008; M. Bojowald, [arXiv:1209.3403 [gr-qc]]
- [3] A. Ashtekar and D. Sloan, *Phys. Lett. B*, 694, 108, 2012; A. Ashtekar and D. Sloan, *Gen. Rel. Grav.*, 43, 3519, 2011
- [4] E. Bianchi, arXiv:1204.5122 [gr-qc]
- [5] J. Mielczarek, *JCAP*, 0811, 011, 2008; J. Grain and A. Barrau, *Phys. Rev. Lett.* 102, 081301, 2009; J. Mielczarek, *Phys. Rev. D*, 79, 123520, 2009; M. Bojowald, G. M. Hosain, M. Kagan and S. Shankaranarayanan, *Phys. Rev. D*, 79 043505, 2009; J. Mielczarek, T. Cailleteau, J. Grain, A. Barrau, *Phys. Rev. D*, 81, 104049, 2010; J. Grain, A. Barrau, T. Cailleteau, J. Mielczarek, *Phys. Rev. D* 82, 123520, 2010; M. Bojowald and G. Calcagni, arXiv:1011.2779 [gr-qc]; M. Bojowald, G. Calcagni and S. Tsujikawa, arXiv:1101.5391 [astro-ph.CO]; E. Wilson-Ewing, *Class. Quant. Grav.* 29 085005, 2012; L. Linsefros, T. Cailleteau, A. Barrau, J. Grain, arXiv:1212.2852 [gr-qc]
- [6] M. Bojowald, *Phys. Rev. Lett* 100, 221301, 2008
- [7] A. Ashtekar, J. Baez, A. Corichi, and K. Krasnov, *Phys. Rev. Lett.* 80, 904, 1998
- [8] J. Mielczarek, M. Kamionka, A. Kurek and M. Szydlowski, *JCAP* 1007, 004, 2010